ELECTRONIC SUPPLEMENTARY MATERIAL

Stochastic transitions in a bistable reaction system on the membrane

Marek Kochańczyk, Joanna Jaruszewicz, and Tomasz Lipniacki

This material features the article published in the *Journal of the Royal Society Interface*, 2013.

Supplementary table

Parameters of the analysed system used in simulations

Parameter	Dimensionless values			Dimensional values for $c_0 = 10/\text{s}$, $\ell = 0.01$ μm
	On-lattice KMC	Gillespie KMC	PDEs	On-lattice KMC
c_0	1.667	$10/V$	1	10/s
c_1	0.008333	$0.05/V$	0.02	0.05/s
c_2	{0.025, 0.0625, 0.08333}	{$0.15/V$, $0.375/V$, $0.5/V$}	{0.06, 0.15, 0.2}	{0.15/s, 0.375/s, 0.5/s}
c_3	1.667	$10/V$	4	10/s
M	18 to 6000	∞	18 to 6000	300 to 10 000/s
D	2.25 to 750	∞	2.25 to 750	3.75×10^{-3} to 1.25 $\mu\text{m}^2/\text{s}$
l	1	—	1	0.01 μm
$\rho_{\mathcal{K}}$	0.4	—	—	$4619/\mu\text{m}^2$
$\rho_{\mathcal{P}}$	0.1	—	—	$1155/\mu\text{m}^2$

TABLE S1: *Parameters of the analysed system.* Parameters are described in the main text. Only c_2 and M (and D) vary between simulations; other parameters, referred to as default parameters in the main text, are the same in all simulations.

Physiological relevance of parameter values used in simulations:

- Rate constants of reactions on the membrane can be as fast as 100/s [S1]; the relation $c_1 < c_2 < c_3$ reflects the strong boost to the catalytic activity of a kinase resulting from the increase in the number of its phosphorylated sites [S2].
- Diffusion coefficients of membrane proteins lie in the range of 10^{-2} to 10^{-1} $\mu m^2/s$ (which is at least an order of magnitude lower than in the cytoplasm) [S3, S4].
- The lattice constant ℓ is assumed to correspond exactly to the average centre-to-centre spacing of neighbouring membrane proteins [S5]. At $\ell = 10$ nm compartment volumes analysed in simulations correspond well to sizes of plasma membrane confinement zones, which e.g. in NRK cells have the mean diameter of about 230 nm as revealed by single-particle tracking experiments [S6]; on the other hand, as we consider isolated chambers, transient trapping of proteins in zones of confinement is not reflected in simulations.
- A significant fraction of the membrane surface can be covered by proteins [S7]. The surface density of membrane proteins is of order of $100/\mu m^2$, but in some cases can be even as high as $10\,000/\mu m^2$ [S8]. (The calculation of dimensional densities of molecules involves the formula for the surface of a hexagon: $A = \frac{\sqrt{3}}{2}\ell^2$.)

Supplementary references:

S1 Faeder, J. R., Hlavacek, W. S., Reischl, I., Blinov, M. L., Metzger, H., Redondo, A., Wofsy, C. & Goldstein, B. 2003 Investigation of early events in FcεRI-mediated signaling using a detailed mathematical model. *J. Immunol.* **170**, 3769–3781.

S2 Alessi, D. R., Saito, Y., Campbell, D. G., Cohen, P., Sithanandam, G., Rapp, U., Ashworth, A., Marshall, C. J. & Cowley, S. 1994 Identification of the sites in MAP kinase kinase-1 phosphorylated by p74raf-1. *EMBO J.* **13**, 1610–1619.

S3 Elowitz, M. B., Surette, M. G., Wolf, P. E., Stock, J. B. & Leibler, S. 1999 Protein mobility in the cytoplasm of Escherichia coli. *J. Bacteriol.* **181**, 197–203.

S4 Ramadurai, S., Holt, A., Krasnikov, V., van den Bogaart, G., Killian, J. A. & Poolman, B. 2009 Lateral diffusion of membrane proteins. *J. Am. Chem. Soc.* **131**, 12650–12656. (doi:10.1021/ja902853g)

S5 Phillips, R., Ursell, T., Wiggins, P. & Sens, P. 2009 Emerging roles for lipids in shaping membrane-protein function. *Nature* **459**, 379–385. (doi:10.1038/nature08147)

S6 Kusumi, A., Nakada, C., Ritchie, K., Murase, K., Suzuki, K., Murakoshi, H., Kasai, R. S., Kondo, J. & Fujiwara, T. 2005 Paradigm shift of the plasma membrane concept from the two-dimensional continuum fluid to the partitioned fluid: high-speed single-molecule tracking of membrane molecules. *Annu. Rev. Biophys. Biomol. Struct.* **34**, 351–378. (doi:10.1146/annurev.biophys.34.040204.144637)

S7 Zhou, H.-X. 2009 Crowding effects of membrane proteins. *J. Phys. Chem. B* **113**, 7995–8005. (doi:10.1021/jp8107446)

S8 Kalay, Z., Fujiwara, T. K. & Kusumi, A. 2012 Confining domains lead to reaction bursts: reaction kinetics in the plasma membrane. *PLoS One* **7**, e32948. (doi:10.1371/journal.pone.0032948)

Supplementary figures

Gillespie algorithm versus on-lattice KMC for large motility

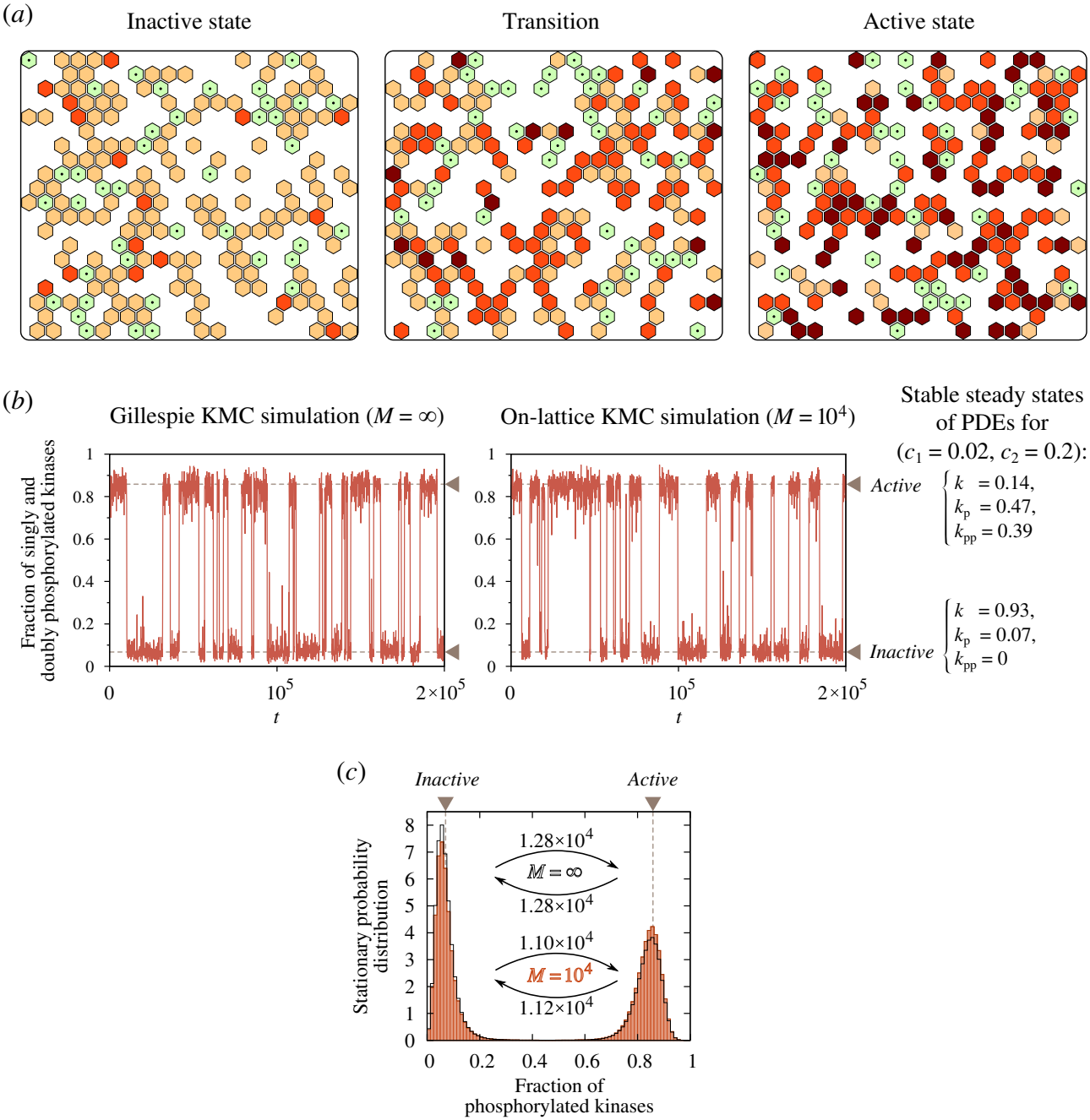

FIGURE S1: *Comparison of KMC on the lattice simulations for large motility coefficient $M = 10^4$ and the corresponding spatially homogeneous Markov process simulated with Gillespie algorithm.* Domain size: 20×20, periodic boundary conditions; parameters: ($c_1 = 0.02$, $c_2 = 0.2$). (*a*) Three snapshots from on-lattice KMC simulations (dephosphorylated kinases – orange, monophosphorylated – red, bisphosphorylated – brown; phosphatases – pale green, marked with a dot). (*b*) Trajectories of the fraction of phosphorylated kinases $k_p + k_{pp}$ from the Gillespie algorithm and on-lattice KMC simulations. (*c*) Bimodal stationary probability distribution of $k_p + k_{pp}$ calculated from long on-lattice (boxes) and Gillespie algorithm (thick black overlay) KMC simulations. MFPTs τ_{on} and τ_{off} are shown for both methods.

Propagation of induced travelling waves in the semi-1-D reactor

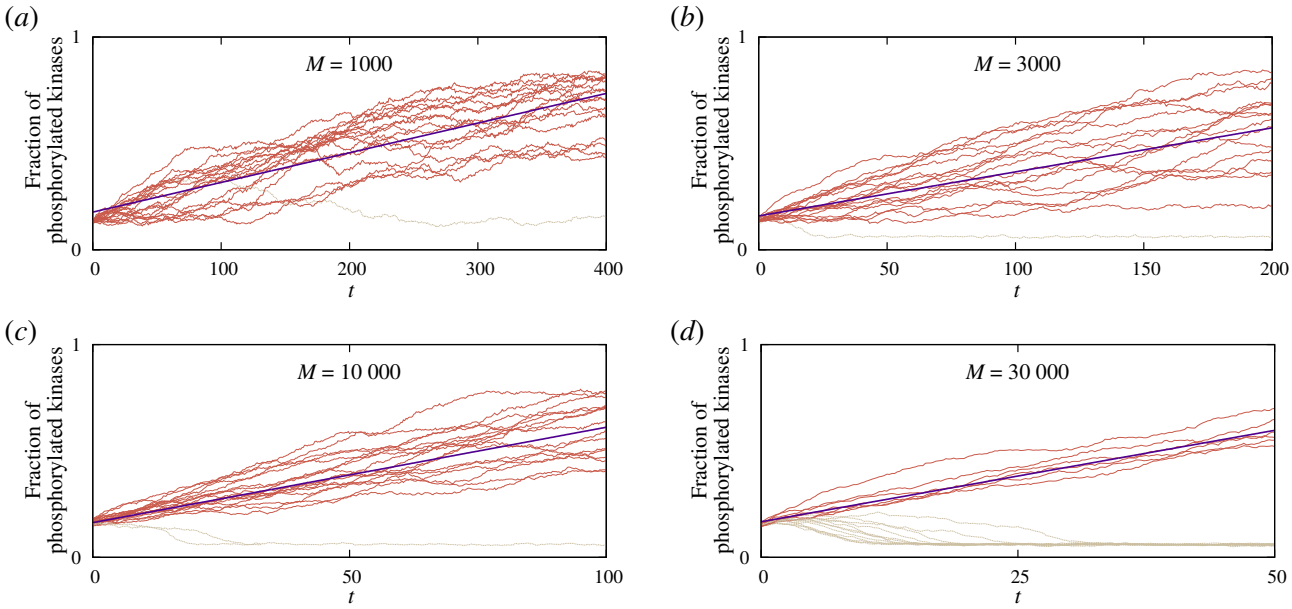

FIGURE S2: *Fraction of phosphorylated kinases $k_p + k_{pp}$ averaged over the whole reactor 30 × 1100 during the induced wave propagation.* Travelling wave velocities shown in figure S3 were estimated from linear fits to these trajectories. When the "seed" had become deactivated, so that the travelling wave did not form, the corresponding trajectory was not taken into account in fitting (dashed pale lines). At higher diffusivities the probability that the initially active area ("seed") is swept away and cannot induce the wave is larger.

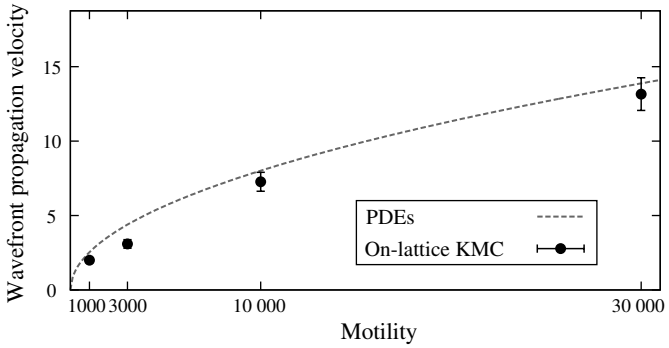

FIGURE S3: *Travelling wave velocity as a function of motility.* Velocities were calculated from simulations of PDEs and estimated in on-lattice KMC simulations for ($c_1 = 0.02$, $c_2 = 0.15$) (figure S2). Error bars – SD.

Coinciding stochastically and deterministically preferred steady states

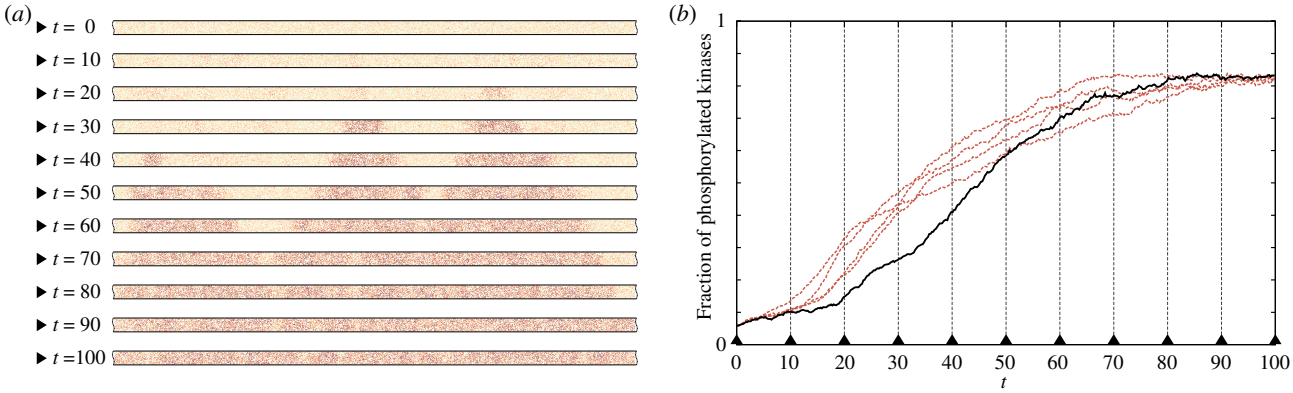

FIGURE S4: *Simultaneous spontaneous activation on the long toroidal domain 30 × 1000.* Parameters: ($c_1 = 0.02$, $c_2 = 0.2$) and $M = 300$. (a) Snapshots from the on-lattice KMC simulation, (b) five example time profiles of phosphorylated kinases $k_\mathrm{p} + k_\mathrm{pp}$. Snapshots in ($a$) correspond to the trajectory represented by the solid black line in (b).

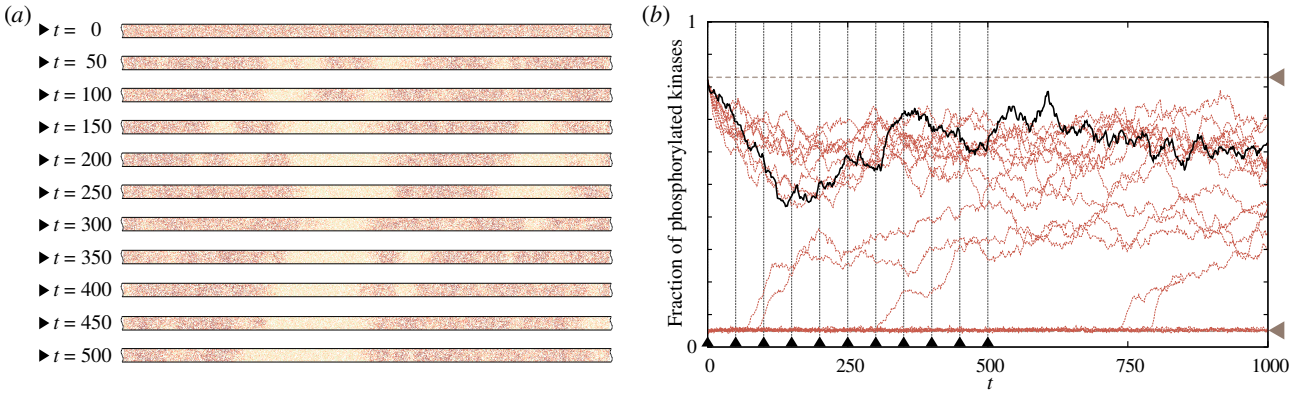

FIGURE S5: *Self-sustaining transient patches of activity in a toroidal domain 30 × 1000.* Parameters: ($c_1 = 0.02$, $c_2 = 0.06$) and $M = 300$. (a) Snapshots from the on-lattice KMC simulation, (b) time profiles of $10 + 10$ trajectories starting from the spatially homogeneous active and inactive steady states (horizontal dashed lines). Snapshots in (a) correspond to the trajectory represented by the solid black line in (b).

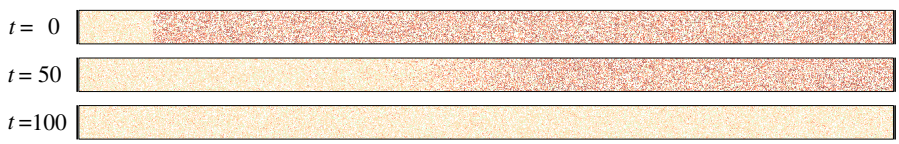

FIGURE S6: *Kinase inactivity wave propagation on the cylindrical domain 50 × 1000 for very large motility $M = 10\,000$.* Three snapshots from an on-lattice KMC simulation. Parameters: ($c_1 = 0.02$, $c_2 = 0.06$).

Activation due to a locally reduced motility

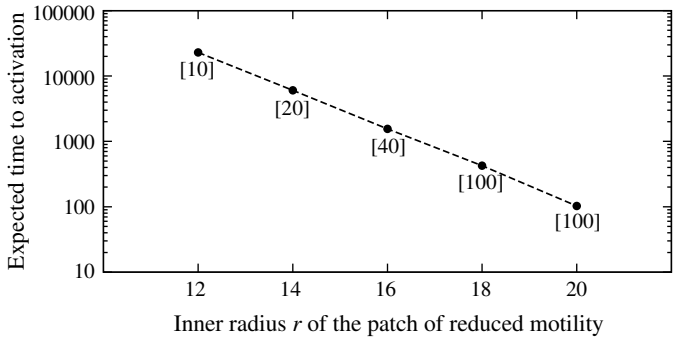

FIGURE S7: *Dependence of the expected time to activation* τ_{on} *on the radius of the patch of lowered motility* $M_{\text{patch}} = 100$ *with the overall motility* $M = 1000$ *obtained from on-lattice KMC simulations.* Parameters: ($c_1 = 0.02$, $c_2 = 0.06$) as in figure 8 in the main text. The expected τ_{on} is estimated based on n_{on} observed switches given in square brackets.

Supplementary movies

Movies are available on-line at:

http://pmbm.ippt.gov.pl/publications/supplementary/Kochanczyk-2013-JRSocInterface-Movies.zip

MOVIE S1: *Activity wave initiation on the square domain due to the locally reduced motility coefficient.* System parameters as in figure 8 in the main text.

MOVIE S2: *Self-sustaining transient patches of activity in a toroidal domain.* All parameters as in figure S5.